ROYAL SOCIETY OF CHEMISTRY

www.rsc.org/crystengcomm

Rare-earth carboxylates, [Ln$_2$(III)(μ$_3$-OH)(C$_4$H$_4$O$_5$)$_2$ (C$_4$H$_2$O$_4$)]. 2H$_2$O [Ln = Ce, Pr and Nd] : Synthesis, Structure and Properties

S R Sushrutha, Srinivasan Natarajan[*]

Framework solids Laboratory, Solid State and Structural Chemistry Unit,

Indian Institute of Science, Bangalore-560012, India.

[*] Corresponding Author: Email: snatarajan@sscu.iisc.ernet.in

Abstract

A new series of inorganic-organic hybrid framework compounds, $Ln_2(\mu_3\text{-}OH)(C_4H_4O_5)_2(C_4H_2O_4)]$. $2H_2O$, (Ln = Ce, Pr and Nd), have been prepared employing hydrothermal method. The structure has malic acid and fumaric acid as a part of the structure. The malate units connect the lanthanide centers forming Ln – O – Ln two-dimensional layers, which are cross-linked by the fumarate units forming the three-dimensional structure. The extra framework water molecules form a dimer and occupy the channels. The water molecules can be reversibly adsorbed. The dehydrated structure did not show any differences in the framework structure/connectivity. The presence of lattice water provide pathway for proton conductivity. The optical studies suggest an up-conversion behavior involving more than one photon for the neodymium compound.

Introduction

Inorganic-organic hybrid framework compounds constitute an important family in the area of materials chemistry.[1] The studies carried out during the last decade or so, concentrated on the use of rigid aromatic linkers to form new frameworks exhibiting interesting properties such as proton conduction, sorption and catalysis.[2] The use of aliphatic dicarboxylic acids for the formation of interesting frameworks have also been attempted.[3,4] The formation of lanthanide carboxylates with robust three-dimensional structures have been known.[3] The studies on transition metal aliphatic carboxylates showed that three dimensional structures with extended $-M - O - M-$ connectivity could be formed through an entropy driven dehydration process.[4,5] In addition, the extended inorganic connectivity in one- or two- dimensions appear to enhance the thermal stability, possibly due to the inertness of the inorganic skeleton.[4c,6]

One of the important issues with regard to the design of new framework compounds employing rare-earth ions is their coordination preferences. Unlike the transition elements, where the coordination ranges from 4 to 6, the rare-earths have coordination numbers in the range of 8 to 12. The higher coordination requirement could be an impediment in designing simple frameworks, but it could be beneficial in stabilizing unusual frameworks as shown in recent years.[7] The other component of the hybrid frameworks, the organic linkers, have undergone a number of modifications. It has been shown that designed organic ligands could be employed to prepare newer framework with precise structures.[8] Rare-earth carboxylates exhibiting a number of structures have also been known[9] Though there have been reasonable interest in the preparation of new compounds containing mixed ligands such as aromatic and heterocyclic,[10] aromatic and aliphatic[11] etc., but the use of two different aliphatic dicarboxylic acids appears to be limited.

We have been investigating the use of two different aliphatic acids in the synthesis of newer hybrid frameworks of rare-earths under hydrothermal conditions. To this end, we have employed malic acid and fumaric acid in the reaction mixture along with rare-earth salts. This study resulted in a new compound $[Ln_2(\mu_3-OH)(C_4H_4O_5)_2(C_4H_2O_4)].2H_2O$, (Ln = Ce, Pr and Nd) with an interesting pillar-layered structure. In this manuscript the synthesis, structure and the properties of the compounds are described and discussed.

Experimental section

Synthesis and Characterization

All the compounds were prepared under hydrothermal conditions. In a typical synthesis, DL-Malic acid (0.133 g, 1 mM), was dissolved in 2 ml water, ethylenediamine (0.020 ml) was added to adjust the pH to 5. $Ce(NO_3)_3.6H_2O$ (0.355 g, 1 mM) was dissolved separately in 2 ml water and added to the malic acid solution. The mixture was homogenised at room temperature for 30 minutes. The resulting solution was transferred to a 15 ml PTFE- lined autoclave and heated at 180°C for 72 hours. The polycrystalline powder product was filtered under vacuum, washed with water and dried under ambient conditions. The Pr, Nd compounds were prepared by reacting $PrCl_3.7H_2O$ or $NdCl_3.6H_2O$. Single crystalline products were obtained for Pr (pale green crystals), Nd (pale-violet crystals). We observed that the use of DL-Aspartic acid as well as fumaric acid in the reaction mixture either independently or in combination also results in the products reported herein. CHN analysis was carried out for all the three compounds. Elemental analysis, Ce-compound: calcd. C 18.34%, H 1.82%; found C 18.27%, H 2.12%; For Pr: calcd. C 18.20%, H 1.81%; found C 18.26%, H 2.19%; for Nd: calcd. C 18.14%, H: 1.81%; found C:18.04%, H:2.06%.

The powder X-ray diffraction (PXRD) patterns were recorded in the 2θ range 5-50° using Cu Kα radiation (Philips X'pert). The experimental PXRD patterns for all the three compounds were consistent with the simulated PXRD patterns generated using the single crystal X-ray structure determined for Pr and Nd compounds (ESI, Figure S1). The IR spectroscopic studies were carried out on KBr pellets (Perkin-Elmer, SPECTRUM 1000). The observation of bands at about 3390 cm^{-1} and 3550cm^{-1} for all the three compounds confirms the presence of lattice water molecules and the hydroxyl groups (ESI, Figure S2, Table S1).[12]

Thermogravimetric analysis (TGA) (Metler-Toledo) was carried out in an oxygen atmosphere (flow rate = 50 ml/min) in the temperature range 30°C – 850°C (heating rate = 5°C/min) for all the three compounds (ESI, Figure S3). The thermal behaviour was found to be similar for the compounds. Te Cd compound exhibited an initial weight loss of 5.8% (calc. 5.5%) in the temperature range of 80°C – 160°C which corresponds to the loss of two lattice water molecules. A small weight loss followed by a larger one was observed in the temperature range 300-580°C [obsd: 45.4% (calc. 44.6)] which could be due to dehydroxylation of malate as well as the loss of the carboxylate moieties. The total observed weight loss for all compounds is as follows: 51.2 (calcd. 50.1%) for Ce,48.2 (calc. 49.9%) for Pr, 47.3 (calc. 48.9%) for Nd. The final calcined products in all the cases were found to be crystalline by PXRD and correspond to their respective oxides.

The UV-vis absorption spectra (Perkin-Elmer model Lambda 35) and the photoluminescence spectra (Perkin-Elmer, LS 55) for the Nd-compound was recorded on a solid sample at room temperature. The characteristic neodymium emissions were observed and are presented in later section.

Conductivity measurement was carried out on a powdered sample for the Pr compound by impedance spectroscopy (Alpha, Novocontrol) in the frequency range 1- 10^6 Hz (signal amplitude: 0.12 V). The sample pellets were sandwitched between two stainless steel electrodes and are exposed to relative humidity of 98% for 24 hours before taking the measurement. There was no any noticeable changes was observed in the PXRD pattern of the sample after exposing to the relative humidity of 98% (ESI Figure S4).

Single-Crystal Structure Determination

A suitable single crystal of Pr and Nd was carefully selected under a polarizing optical microscope and glued to the thin glass fibre. The single crystal data were collected with a Bruker AXS Smart Apex CCD diffractometer at 293 K. The data for the dehydrated compound of Pr was collected at 393K under *in situ* conditions. The X-ray generator (Mo Kα) was operated at 50 kV and 35 mA. Data were collected with ω scan width of 0.3°. A total of 606 frames were collected at three different settings of φ (0, 90, 180°) keeping the sample-to-detector distance fixed at 6.03 cm and the detector position (2θ) fixed at −25°. The data were reduced using SAINTPLUS[13] and an empirical absorption correction was applied using the SADABS program.[14] The structure was solved by direct methods and refined using SHELX97[15] present in the WinGX suit of programs (version 1.63.04a).[16] The final refinement included atomic position for all the atoms and anisotropic thermal parameters for all the non-hydrogen atoms. The full matrix least square refinement against $|F^2|$ was carried out using WinGx package of programs.[16] By using atomic coordinates of the Pr compound, structure factor amplitude was extracted by using Le Bail method for the Ce compound (ESI, Table S2, Figure S5). [17] The CCDC numbers for the compound Pr, dehydrated Pr and Nd compounds are 969256, 969257 and 969258, which can be obtained free of charge from Cambridge Crystallographic Data Center (CCDC) *via* www.ccdc.cam.ac.uk.

Results and Discussion

Structure of $[Ln_2(\mu_3\text{-OH})(C_4H_4O_5)_2(C_4H_2O_4)].2H_2O$ (Ln = Ce, Pr and, Nd)

From the powder XRD patterns, it was clear that all the three compounds have the same structure (ESI Figure S1). Good quality single crystals were obtained only in the case of Pr and Nd. For the purpose of

structural description, the single crystal structure of the Pr compound is presented here. The asymmetric unit has two crystallographically independent Pr atoms [Pr(1) and Pr(2)], one μ_3-OH, two distinct malate ions (malate-1 and malate-2), half a fumarate ion and two lattice water molecules (ESI, Figure S6). The Pr(1) is ten coordinated with a bi-capped square anti-prismatic geometry (ESI, Figure S7a) and Pr(2) is nine coordinated with a tricapped trigonal prismatic geometry (ESI, Figure S7b). The Pr — O bond distances are in the range from 2.402(3) Å to 2.696(3) Å (av. 2.549Å) (Table2). The carboxylate groups exhibit three different binding modes viz., μ_3-η^2:$\eta^1$and μ_3-η^2:η^2 modes, bridging three metal centres and μ_2-η^2:η^1 modes, bridging two metal centres (ESI, figure S7c).

The structure can be explained by considering the connectivity between the Pr polyhedra. Thus, Pr(1) atoms are connected through μ_3—oxygens [O(7) and O(7)$^{\#1}$] forming Pr_2O_{18} edge-shared dimers. The dimers are linked further by the μ_2—oxygens [O(2) and O(2)$^{\#2}$] forming a one-dimensional Pr — O — Pr chains (Figure 1a). Pr(2) atoms also form a Pr_2O_{16} dimeric units through μ_2 — oxygens [O(9) and O(9)$^{\#3}$]. The dimers are linked to the one-dimensional Pr — O chains via the μ_3 — oxygen [O(7)] forming a two-dimensional extended Pr — O — Pr oxide layers (Figure 1b) (ESI, Figure S8). The Pr centers are separated by distances in the range of 4.11 – 4.21Å. The malate units occupy the spaces in between the Pr units forming the hydrophobic region (ESI, Figure S9). The lanthanide oxide layers are pillared by the other carboxylate, fumarate, forming the three-dimensional structure (Figure 1c) (ESI, Figure S10). The three-dimensional structure encompasses two types of hydrophilic channels (5.3 × 4.5Å along a-axis and 7.5× 5Å along b-axis; atom-atom contact distances not including the van der Waals radii) in which the lattice water molecules are located (Figure 2a). The lattice water molecules also participate in hydrogen bond interactions. Thus O — H . . . O hydrogen bonds have been observed in the present structure (Table 3). The two sets of water molecules [O(14) and O(15)] forms a dimer and have weak interactions leading to a one dimensional water chains that are separated by distances in the range of 2.8 − 3.1 Å (within the dimer) and 3.2 −4.2Å (inter-dimer) (Figure 2b). Similar water chains have also been observed previously in the supramolecularly organised channel structures of cyanuric acid and melamine.[18] It may be noted that the Ln — O — Ln two dimensional networks are formed entirely through the malate carboxylate oxygens. Thus, one can define this structure as I^2O^1 type – inorganic in two-dimensions and organic in one-dimension.[6]

Formation of lanthanide aliphatic carboxylates have been observed earlier.[3] Ferey and co-workers have described the formation of many rare-earth carboxylates.[3] Of these, the present structure has close relationship

with the structures formed employing the succinate and glutarate ones.[3d,e] In the praseodymium succinate structure, $[Pr(C_4H_4O_4)_3(H_2O)_2] \cdot H_2O$, the one-dimensional — Ln — O — Ln — chains are connected by the succinate carboxylate units forming the two- and three- dimensional structure (ESI, Figure S11). In the present structure, the presence of the –OH group and its participation in bonding with the lanthanide ions gives rise to a two-dimensional — Ln — O — Ln — arrangement. Two-dimensional — M — O — M — oxide layers pillared by succinate units, have been observed in cobalt succinate, $[Co_5(OH)_2(C_4H_4O_4)_4]$,[4h] which appears to be more closely related to that observed in the present structure (ESI, Figure S12).

In situ formation of ligand:

During the synthesis of the compound $[Pr_2(\mu_3\text{-}OH)(C_4H_4O_5)_2(C_4H_2O_4)].2H_2O$, the initial reaction conditions were similar and comparable to those employed for the preparation of $[Pr(C_4H_4O_4)_3(H_2O)_2] \cdot H_2O$, MIL-17.[3d] The initial acid employed was malic acid, but the final product contained both the malate as well as the fumarate anions. The formation of fumarate moieties from the malate can be explained by a simple dehydration step under hydrothermal conditions. It may be noted that formation of new intermediates, new reactants have been observed during the synthesis of many open framework compounds.[19] We have attempted the synthesis of the title compounds by employing a reaction mixture containing malic acid and fumaric acid, which also resulted in the same compounds reported herein (ESI, Table S4). In order to expand the scope of the present investigation, we have also attempted reactions employing aspartic acid, malic acid and fumaric acid both independently as well as in combination of any two acids (ESI, Table S4). In most of the preparations, we have observed the formation of the present compounds. The formation of the malate and fumarate anions from the aspartate anions as well as the formation of malate anion from fumarate anions can be explained employing simple organic reaction mechanistic steps (ESI, Scheme S1, 2).

Thermal Stability and Recyclability

From the TGA studies, it appears that the solid loss the lattice water molecules in the temperature range of 80 – 160°C. The TGA studies also suggest that the structure could be retained up to 250°C. In order to verify this, we have carried out *in-situ* variable temperature PXRD studies. From the PXRD studies, it is clear that the present structure is stable up to 250°C, though the structural collapse was observed for higher temperatures leading to a X-ray amorphous product (ESI, Figure S13). We have also carried out *in-situ* single crystal XRD studies at 120°C to probe the possible changes that accompany the dehydration of the sample. The single crystal XRD studies demonstrate that the overall three-dimensional structure remains the same, but the

lattice water molecules removed, resulting in ~14% void within the framework (Figure 2a). The water molecules were re-adsorbed on exposure to atmospheric conditions over a period of 24 hours.

This recyclability of water adsorption/desorption was also examined by employing TGA studies (Figure 3). For this, the TGA set-up was modified to introduce the saturated water vapour. Initially, the sample was heated up to 140°C in a flow of dry N_2 (50 ml/min) and held for 30 minutes. The dehydrated sample was cooled to room temperature and water vapour was introduced to the system for rehydration for 45 minutes. During this step, the sample appears to regain most of the original weight (~99%). This step of dehydration/rehydration was repeated three times with similar behaviour. This observation suggests that the present compounds have reasonably stable 3D network.

Water adsorption studies have also been carried out using Belsorp-Aqua 3 analyser on samples pre-treated at 120°C for 4 hours (Figure 4). The water adsorption studies indicate rapid water up take at low partial pressures, which is suggestive of solids having micropores. The sample did not exhibit any profound hysteresis which also indicates that the water adsorption /removal is facile. Cyclic TGA studies also points towards similar behaviour. The total adsorbed water corresponds to ~1.9 mole of water, which is close to that observed from the TGA and single crystal XRD studies.

Proton Conductivity Studies

The presence of water dimers and weakly interacting water chains in the channels having O −H . . . O hydrogen bonds along with the complete recyclability suggested the possibility of probing the proton conductivity behaviour in these compounds. Thus, AC impedance studies were carried out under a relative humidity of 98%. From the Nyquist plots, proton conductivity values of 2.8×10^{-6} S cm^{-1} was observed for the Pr −compound (Figure 5a). This value is similar to that observed earlier in $[M(C_8H_6O_4)(OH)(H_2O)]$ (M= Al, Fe), MIL-53.[20] As mentioned above, the two water molecules have strong hydrogen bond interactions, which would provide the necessary pathway for the migration of protons through the Grotthus mechanism (Figure 2b). The activation energy calculated from the Arrhenius plot gave a value of 0.5 eV, which is also suggestive of Grotthus mechanism for proton transport in the compound (Figure 5b).

Optical studies

Up-conversion studies on $[Nd_2(\mu_3\text{-OH})(C_4H_4O_5)_2(C_4H_2O_4)]\cdot 2H_2O$:

Lanthanide compounds exhibit interesting optical behavior due to ligand sensitized and sharp *f-f* emissions. Among the lanthanide ions, Eu^{3+} and Nd^{3+} are important due to their emission in the visible region (Eu^{3+}) (λ=500-700 nm) and in the near IR region (Nd^{3+}) (λ=800-1700 nm). In addition it has been shown that the Nd compounds can exhibit up-conversion behavior of converting the IR radiation into visible region, through a two –photon absorption process.[21] Conversion of longer wavelength radiation into shorter wavelength require multi-photon process. Trivalent lanthanide ions have been investigated as possible host for such up-conversion behavior due to the availability of a number of electronic states.[22] There have been some attempts in the literature on the exploratory study of Nd-containing compounds for the up-conversion behavior.[23]

As a part of this study, we have explored the possible multi-photon absorption behavior of the Nd compound, $[Nd_2(\mu_3\text{-}OH)(C_4H_4O_5)_2(C_4H_2O_4)].2H_2O$. The UV-vis spectra of the compound (Figure 6a) exhibit good stark splitting of the higher states due to the crystal-field effects.[24] The UV-vis spectra could not be resolved completely due to the overlap of the excited and ground state stark levels. A schematic of the possible energy transition states during the up-conversion process employing the Nd^{3+} ion is shown in Figure 6b. Of these, the absorption band corresponds to the $^4I_{9/2} \rightarrow {}^4G_{5/2}$ appears to be attractive for the investigation of up-conversion behavior. Thus, an excitation wavelength of λ=580 nm was chosen as it is far removed from the intra-ligand absorption bands. Three distinct emission bands corresponding to $^4D_{3/2} \rightarrow {}^4I_{11/2}$ (365 nm), $^4D_{3/2} \rightarrow {}^4I_{13/2}$ (424 nm), $^4D_{3/2} \rightarrow {}^4I_{15/2}$ (434 nm) transitions were observed (Figure 7). It may be noted that the direct excitation to $^4D_{3/2}$ or $^4D_{5/2}$ levels are generally difficult as they are closer to the intra-ligand absorption bands and hence must undergo a transfer from the $^4F_{3/2}$ levels. Thus, it is believed that the excitation wavelength (λ=580 nm) would normally populate the $^4F_{3/2}$ levels, which would be subsequently re-excited to reach $^4D_{3/2}$ or $^4D_{5/2}$ levels (Figure 6b).

To evaluate whether the current absorption behavior of the Nd-compound has the involvement of two photons are not, we have carried out a number of similar experiments. To this end, a series of sterile glass plates were placed sequentially in the path between the source and the sample. This would decrease the intensity of the light source and also the transmitted light through the sample (Figure 8a). One can carry out this experiment both in the absence as well as in the presence of the sample and a simple correlation can be arrived.

Accordingly, if n is the number of photons involved, then,

$$I_{em} \; \alpha \; (I_{ex})^n$$

$$I_{em} = A \, (I_{ex})^n$$

$$\log I_{em} = A + n \log I_{ex}$$

The value of n can be obtained from the log-log plot of I_{em} Vs I_{ex}. The result of this study is shown in Figure 8b. A simple fit of the observed line gives a value for n in the range of $1.3 - 1.46$ (Figure 8b). The dehydrated compound also showed similar type of behavior (ESI, Figure S14, 15). This suggests that the emission from the $^4D_{3/2}$ state involves more than one photon. Normally, one would expect to have a value closer to 2 for n, if the emission involved in two photon absorption. It is likely that the population of the $^4D_{3/2}$ level is not sufficiently high and there could be considerable loss through non-radiative decay involving a number of intermediate energy levels.

Conclusions

The synthesis, structure and characterization of a family of new inorganic-organic hybrid framework compounds, $Ln_2(\mu_3\text{-}OH)(C_4H_4O_5)_2(C_4H_2O_4)].2H_2O$; (Ln = Ce, Pr and Nd), involving two distinct organic ligands has been accomplished. The facile removal/reinsertion of lattice water molecules from the structure is suggestive of reasonable robustness for the three-dimensional framework. The lattice water molecules form a dimer and weak inter-dimer interactions, provide a pathway for the migration of protons with conductivity values of 2.85×10^{-6} S cm^{-1} at 98% relative humidity. Optical study indicates that the Nd^{3+} compound exhibit an up-conversion behaviour involving more than one-photon when excited using λ=580 nm wavelength. The present studies clearly suggest that it would profitable to explore inorganic-organic hybrids that involve multiple carboxylic acids. We are presently pursuing this theme.

Acknowledgement

References

1. Special issue on MOFs: (a) *Chem. Rev.,* 2012, **112**, 675-1268; (b) *Chem. Soc. Rev.,* 2009, **38**, 1201-1508; (c) *Eur. J. Inorg. Chem.,* **2010**, *24*, 3683-3874; (d) S. Horike, D. Umeyama, and S. Kitagawa, *Acc. Chem. Res.,* 2013; (e) W. Xuan, C. Zhu, Y. Liu and Y. Cui, *Chem. Soc. Rev.,* 2012, **41**, 1677.

2. (a) M. Yoon, K. Suh, S. Natarajan and K. Kim, *Angew. Chem., Int. Ed.,* 2013, **52**, 2688; (b) J. M. Taylor, K. W. Dawson and G. K. H. Shimizu, *J. Am. Chem. Soc.,* 2013, **135**, 1193; (c) T. Kundu, S. C. Sahoo and R. Banerjee, *Chem. Commun.,* 2012, **48**, 4998; (d) T. Panda, T. Kunduz and R. Banerjee, *Chem. Commun.,* 2012, **48**, 5464; (e) A. Shigematsu, T. Yamada and H. Kitagawa, *J. Am. Chem. Soc.,* 2011, **133**, 2034; (f) W. M. Bloch, R. Babarao, M. R. Hill, C. J. Doonan and C. J. Sumby, *J. Am. Chem. Soc.,* 2013, **135**, 10441; (g) R. Vaidhyanathan, S. S. Iremonger, G. K. H. Shimizu, P. G. Boyd, S. Alavi and T. K. Woo, *Angew. Chem. Int. Ed.,* 2012, **51**, 1826; (h) Y. X. Tan, Y. P. He and J. Zhang, *Chem. Commun.,* 2011, **47**, 10647; (i) P. V. Dau and S. M. Cohen, *Chem. Commun.,* 2013, **49**, 6128; (j) Q. Han, C. He, M. Zhao, B. Qi, J. Niu, and C. Duan, *J. Am. Chem. Soc.,* 2013, **135**, 10186; (k) M. Gustafsson, A. Bartoszewicz, B. M. Matute, J. Sun, J. Grins, T. Zhao, Z. Li, G. Zhu and X. Zou, *Chem. Mater.,* 2010, **22**, 3316.

3. (a) C. Serre, F. Pelle, N. Gardant and G. Ferey, *Chem. Mater.,* 2004, **16**, 1177; (b) C. Serre, J. Marrot, and G. Ferey, *Inorg. Chem.,* 2005, **44**, 654; (c) F. Millange, C. Serre, J. Marrot, N. Gardant, F. Pelle and G. Ferey, *J. Mater. chem.,* 2004, **14**, 642; (d) F. Serpaggi and G. Ferey, *Microporous and Mesoporous Mater.,* 1999, **32**, 311; (e) F. Serpaggi and G. Ferey, *J. Mater. Chem.,* 1998, **8**, 2737; (f) G. Zhang, G. Yang and J. S. Ma, *Cryst. Growth Des.,* 2006, **6**, 933.

4. (a) C. Livage, C. Egger and G. Ferey, *Chem. Mater.,* 1999, **11**, 1546; (b) Y. Kim, E. Lee and D. Y. Jung, *Chem. Mater.,* 2001, **13**, 2684; (c) P. M. Forster and A. K. Cheetham, *Angew. Chem., Int. Ed.,* 2002, **41**, 457; (d) E. Lee, Y. Kim and D. Y. Jung, *Inorg. Chem.,* 2002, **41**, 501; (e) R. Vaidhyanathan, S. Natarajan, and C. N. R. Rao, *Cryst. Growth Des.,* 2003, **3**, 47; (f) P. M. Forster, N. Stock and A. K. Cheetham, *Angew. Chem., Int. Ed.,* 2005, **44**, 7608; (g) P. J. Saines, B. C. Melot, R. Seshadri and A. K. Cheetham, *Chem. Eur. J.,* 2010, **16**, 7579; (h) C. Livage, C. Egger, M. Nogues and G. Ferey, *J. Mater. Chem.,* 1998, **8**, 2743.

5. (a) P. Mahata, A. Sundaresan and S. Natarajan, *Chem. Commun.,* 2007, 4471; (b) P. Mahata, M. Prabu, and S. Natarajan, *Inorg. Chem.,* 2008, **47**, 8451; (c) P. M. Forster, A. R. Burbank, C. Livage, G. Ferey

and A. K. Cheetham, *Chem . Commun.,* 2004, 368; (d) M. L. Tong, S. Kitagawa, H. C. Chang and M. Ohba, *Chem. Commun.,* 2004, 418.

6. A. K. Cheetham, C. N. R. Rao and R. K. Feller, *Chem. Commun.,* 2006, 4780.

7. (a) H. Li, W. Shi, K. Zhao, Z. Niu, H. Li and P. Cheng, *Chem. Eur. J.,* 2013, **19**, 3358; (b) X. Feng, J. Wang, B. Liu, L. Wang, J. Zhao and S. Ng, *Cryst. Growth Des.,* 2012, **12**, 927; (c) P. Mahata, K. V. Ramya and S. Natarajan, *Chem. Eur. J.,* 2008, **14**, 5839; (d) F. Gandara, V. A. de la Pena-O'Shea, F. Illas, N. Snejko, D. M. Proserpio, E. G. Puebla and M. A. Monge, *Inorg. Chem.,* 2009, **48**, 4707; (e) Z. Q. Jiang, G. Y. Jiang, D. C. Hou, F. Wang, Z. Zhao and J. Zhang, *CrystEngComm.,* 2013, **15**, 315.

8. (a) R. L. Sangz and L. Xu, *Chem. Commun.,* 2013, **49**, 8344; (b) D. X. Xue, A. J. Cairns, Y. Belmabkhout, L. Wojtas, Y. Liu, M. H. Alkordi and M. Eddaoudi, *J. Am. Chem. Soc.,* 2013, **135**, 7660; (c) M. L. Ma, C. Ji and S. Q. Zang , *Dalton Trans.,* 2013, **42**, 10579; (d) Y. He, H. Furukawa, C. Wu, M. O'Keeffe, R. Krishna and B. Chen, *Chem. Commun.,* 2013, **49**, 6773; (e) T. Devic, C. Serre, N. Audebrand, J. Marrot and G. Ferey, *J. am. chem. soc.,* **2005**, 127, 12788.

9. (a) A. Michaelides, S. Skoulika and M. G. Siskos, *Chem. Commun.,* 2013, **49**, 1008; (b) A. Michaelides, S. Skoulika and M. G. Siskos, *Chem. Commun.,* 2011, **47**, 7140; (c) J. Rocha, L. D. Carlos, F. A. Almeida Paz and D. Ananias, *Chem. Soc. Rev.,* 2011, **40**, 926; (d) Y. Cui, H. Xu, Y. Yue, Z. Guo, J. Yu, Z. Chen, J. Gao, Y. Yang, G. Qian and B. Chen, *J. Am. Chem. Soc.,* 2012, **134**, 3979; (e) H. Li, W. Shi, K. Zhao, Z. Niu, H. Li and P. Cheng, *Chem. Eur. J.,* 2013, **19**, 3358. (f) S. Thushari, A. K. Cha, H. Y. Sung, S. Y. Stephen, L. F. Leung, Y. F. Yen and I. D. Williams, *Chem. Commun.,* 2005, 5515; (g) Z. Amghouz, S. G. Granda and J. R. Garcia, *Inorg. Chem.,* 2012, **51**, 1703; (h) Z. G. Jiang, Y. Kang , J. W. Cheng, Y. L. Feng, *J. Solid State Chem.,* 2012, **185**, 253; (i) Y. Wang, G. X. Liu, Y. C. Chen, K. B. Wang, S. G. Meng, *Inorg. Chim. Acta.* 2010, **363**, 2668.

10. (a) B. Cai, Y. Ren, H. Jiang, D. Zheng, D. Shi, Y. Qian and J. Chen, *CrystEngComm.,* 2012, **14**, 5285; (b) R. F. D'Vries, M. Iglesias, N. Snejko, E. G. Puebla and M. A. Monge, *Inorg. Chem.,* 2012, **51**, 11349; (c) Q. Y. Liu, Z. J. Xiahou, Y. L. Wang, L. Q. Li, L. L. Chen and Y. Fu, *CrystEngComm.,* 2013, **15**, 4930; (d) X. Zhang, L. Fan, Z. Sun, W. Zhang, D. Li, J. Dou and L. Han, *Cryst. Growth Des.,* 2013, **13**, 79; (e) L. Wen, L. Zhou, B. Zhang, X. Meng, H. Qu and D. Li, *J. Mater. Chem.,* 2012, **22**, 22603.

11. (a) X. Feng, J. Wang, B. Liu, L. Wang, J. Zhao and S. Ng, *Cryst. Growth Des.,* 2012, **12**, 927; (b) C. G. Wang, Y. H. Xing, Z. P. Li, J. Li, X. Q. Zeng, M. F. Ge and S. Y. Niu, *Cryst. Growth Des.,* 2009, **9**,

1525; (c) C. G. Wang, Y. H. Xing, Z. P. Li, J. Li, X. Q. Zeng, M. F. Ge and S. Y. Niu, *J. Mol. Struct.,* 2009, **921**, 126; (d) E. C. Yang, H. K. Zhao, B. Ding, X. G. Wang and X. J. Zhao, *Cryst. Growth Des.,* 2007, **7**, 2009.

12. K. Nakamoto, *Infrared and Raman Spectra of Inorganic and Coordination Compounds;* Wiley – Interscience, New York, 2009.

13. SMART (V 5.628), SAINT (V 6.45a), XPREP, SHELXTL, Bruker AXS Inc., Madison, Wisconsin, USA, 2004.

14. G. M. Sheldrick, *Siemens area correction absorption correction program, University of Göttingen, Göttingen, Germany,* 1994.

15. G. M. Sheldrick, *SHELXL-97 program for crystal structure solution and refinement, University of Göttingen, Göttingen, Germany,* 1997.

16. J. L. Farrugia, WinGx suite for small-molecule single crystal crystallography. *J. Appl. Crystallogr.,* 1999, **32**, 837.

17. A. Le Bail, H. Duroy, J. L. Fourquet, *Mater. Res. Bull.,* 1988, **23**, 447.

18. A. Ranganathan, V. R. Pedireddi and C. N. R. Rao, *J. Am. Chem. Soc.,* 1999, **121**, 1752.

19. (a) R. Vaidhyanathan, S. Natarajan and C. N. R. Rao, *Chem. Mater.,* 2001, **13***,* 185; (b) R. H. Jones, A. Chippindale, S. Natarajan and J. M. Thornas, *J. Chem. Soc. Chem. Commun.,* 1994, 565.

20. A. Shigematsu, T. Yamada and H. Kitagawa, *J. Am. Chem. Soc.,* 2011, **133**, 2034.

21. G. Blasse, B. C. G. maier, *Luminescent Materials*, Springer, Berlin, 1994.

22. F. Auzel, *Chem. Rev.,* 2004, **104**, 139.

23. (a) P. Mahata, K. V. Ramya and S. Natarajan, *Chem. Eur. J.,* 2008, **14**, 5839; (b) J. Yang, Q. Yue, G. D. Li, J. J. Cao, G. H. Li and J. S. Chen, *Inorg. Chem.,* 2006, **45**, 2857; (c) B. Yotnoi, A. Rujiwatra, M. L. P. Reddy, D. Sarma and S. Natarajan, *Cryst. Growth Des.,* 2011, **11**, 1347; (d) P. Mahata, K. V. Ramya and S. Natarajan, *Dalton Trans.*, 2007, 4017; (e) D. Sarma, M. Prabu, S. Biju, M. L. P. Reddy and S. Natarajan, *Eur. J. Inorg. Chem.* 2010, 3813.

24. J. J. Ju, T. Y. Kwon, H. K. Kim, J. H. Kim, S. C. Kim, M. Cha, S. I. Yun, *Mater. Lett.,* 1996, **29**, 13.

Figure captions

Fig. 1   (a) View of the one-dimensional Pr — O — Pr chains formed by the linkages between Pr(1) centers

and oxygan atoms in [Pr$_2$(μ_3-OH)(C$_4$H$_4$O$_5$)$_2$(C$_4$H$_2$O$_4$)].2H$_2$O

(b) The two-dimensional Pr — O — Pr inorganic layer formed by the connectivity between the Pr

centers..

(c) The three-dimensional structure of [Pr$_2$(μ_3-OH)(C$_4$H$_4$O$_5$)$_2$(C$_4$H$_2$O$_4$)].2H$_2$O. Note that the fumarate

units pillar the Pr — O — Pr layers.

Fig. 2   (a) View of the three dimensional structure along the b-axis.

(b) View of the water dimer and the weakly interacting water chains in the present compounds.

Fig. 3   Cyclic TGA study showing the reversibility of water adsorption in the Pr compound. Blue curve

represent the heating and cooling cycle and red curve represent the weight loss and gain.

Fig. 4   Water vapour adsorption and desorption isotherm for the Pr compound.

Fig. 5   (a) The Nyquist plot for proton conductivity of [Pr$_2$(μ_3-OH)(C$_4$H$_4$O$_5$)$_2$(C$_4$H$_2$O$_4$)].2H$_2$O under 98%

humidity.

(b) The Arrhenius plot for the proton conductivity for the Pr compound.

Fig. 6   (a) Room-temperature UV-vis absorption spectrum for the [Nd$_2$(μ_3-OH)(C$_4$H$_4$O$_5$)$_2$(C$_4$H$_2$O$_4$)].2H$_2$O.

(b) The schematic energy level diagram for the Nd^{3+} ion showing the various possible transitions

during the up-conversion process.

Fig. 7   Up-converted luminescence spectra of Nd compound recorded at room temperature (λ_{exc}= 580 nm).

Fig. 8   (a) The observed emission dependence on the excitation intensity for [Nd$_2$(μ_3-OH)(C$_4$H$_4$O$_5$)$_2$

(C$_4$H$_2$O$_4$)].2H$_2$O. (a) 100%, (b) 88.88%, (c) 78.18%, (d) 74.48%, (e) 62.965, (f) 56.37%.

(b) The log-log plots of the excitation intensity dependence of the luminescence intensity for the three

emission wavelengths (365 nm, 424 nm, 434 nm).

Table 1. Crystal data and structure refinement parameters for $[Pr_2(\mu_3\text{-OH})(C_4H_4O_5)_2(C_4H_2O_4)].2H_2O$, $[Pr_2(\mu_3\text{-OH})(C_4H_4O_5)_2(C_4H_2O_4)]$, and $[Nd_2(\mu_3\text{-OH})(C_4H_4O_5)_2(C_4H_2O_4)].2H_2O$.

Structural Parameter	Pr	Pr (dehydrated)	Nd
Empirical formula	$C_{10}H_{14}O_{15}Pr_2$	$C_{10}H_9O_{13}\ Pr_2$	$C_{10}H_{10}O_{15}Nd_2$
Formula Weight	656.03	618.99	658.66
Crystal System	Triclinic	Triclinic	Triclinic
Space group	*P-1* (no.2)	*P-1* (no.2)	*P-1* (no.2)
Wavelength (Å)	0.71073	0.71073	0.71073
T/K	293(2)	393(2)	293(2)
a/Å	8.306(4)	8.255(5)	8.249(4)
b/Å	9.343(4)	9.391(6)	9.311(4)
c/Å	11.737(5)	11.616(8)	11.695(6)
A (°)	79.24(2)	80.24(6)	79.30(4)
B (°)	70.49(2)	70.48(6)	70.32(4)
γ (°)	75.92(2)	75.33(5)	76.04(4)
Volume/Å	827.4(6)	817.7(9)	815.5(7)
Z	2	2	2
ρ_{calc} (g/cm^{-3})	2.633	2.514	2.682
μ/mm^{-1}	5.901	5.954	6.378
Θ range (deg)	1.85 – 25.99	2.68 – 25	2.67 – 26
R_{index} (I > 2σ)	$R_1 = 0.0276$, $wR_2 = 0.0763$	$R_1 = 0.0365$, $wR_2 = 0.0825$	$R_1 = 0.0278$, $wR_2 = 0.0600$
R (all data)	$R_1 = 0.0315$, $wR_2 = 0.0792$	$R_1 = 0.0314$, $wR_2 = 0.0781$	$R_1 = 0.0243$, $wR_2 = 0.0578$

$R_1 = \sum | Fo | - | Fc |/\sum | Fo |$; $wR_2 = \{\sum [w (Fo^2 - Fc^2)]/ \sum [w (Fo^2)^2]\}^{1/2}$. $w = 1/[\rho^2(Fo)^2 + (aP)^2 + bP]$. $P = [max (Fo,O) + 2(Fc)^{-2}]/3$ where a = 0.0465and b = 0.2026 for Pr, a = 0.0497and b = 0.0000 for Pr (dehydrated)**,** a = 0.0289 and b = 0.0000for Nd

Table 2: Selected observed bond distances in the compounds $[Pr_2(\mu_3\text{-OH})(C_4H_4O_5)_2(C_4H_2O_4)].2H_2O$, $[Pr_2(\mu_3\text{-OH})(C_4H_4O_5)_2(C_4H_2O_4)]$ and $[Nd_2(\mu_3\text{-OH})(C_4H_4O_5)_2(C_4H_2O_4)].2H_2O$.

| Bond	Distance	Bond	Distance
Pr Compound			
Pr(1)-O(1)	2.538(3)	Pr(2)-O(5)#1	2.696(3)
Pr(1)-O(2)	2.539(3)	Pr(2)-O(6)	2.579(3)
Pr(1)-O(2)#2	2.544(3)	Pr(2)-O(7)	2.411(3)
Pr(1)-O(3)	2.509(3)	Pr(2)-O(8)	2.462(3)
Pr(1)-O(4)	2.659(3)	Pr(2)-O(9)	2.472(3)
Pr(1)-O(5)	2.609(3)	Pr(2)-O(9)#3	2.532(3)
Pr(1)-O(6)	2.568(3)	Pr(2)-O(10)	2.460(3)
Pr(1)-O(7)	2.458(3)	Pr(2)-O(11)	2.555(3)
Pr(1)-O(7)#1	2.530(3))	Pr(2)-O(12)	2.402(3)
Pr(1)-O(8)	2.676(3)		
Pr (dehydrated) compound			
Pr(1)-O(1)	2.566(4)	Pr(2)-O(5)#1	2.671(4)
Pr(1)-O(2)	2.524(4)	Pr(2)-O(6)	2.586(3)
Pr(1)-O(2)#2	2.529(4)	Pr(2)-O(7)	2.408(4)
Pr(1)-O(3)	2.639(4)	Pr(2)-O(8)	2.480(4)
Pr(1)-O(4)	2.496(4)	Pr(2)-O(9)	2.466(4)
Pr(1)-O(5)	2.670(4)	Pr(2)-O(9)#3	2.541(4)
Pr(1)-O(6)	2.563(3)	Pr(2)-O(10)	2.468(4)
Pr(1)-O(7)	2.468(4)	Pr(2)-O(11)	2.642(4)
Pr(1)-O(7)#1	2.509(4)	Pr(2)-O(12)	2.353(4)
Pr(1)-O(8)	2.713(4)		
Nd Compound			
Nd(1)-O(1)	2.528(4)	Nd(2)-O(5)#1	2.674(3)
Nd(1)-O(2)	2.522(4)	Nd(2)-O(6)	2.557(3)
Nd(1)-O(2)#2	2.526(3)	Nd(2)-O(7)	2.396(3)
Nd(1)-O(3)	2.507(4)	Nd(2)-O(8)	2.446(3)
Nd(1)-O(4)	2.646(4)	Nd(2)-O(9)	2.455(3)
Nd(1)-O(5)	2.593(4)	Nd(2)-O(9)#3	2.514(3)
Nd(1)-O(6)	2.557(3)	Nd(2)-O(10)	2.440(3)
Nd(1)-O(7)	2.443(4)	Nd(2)-O(11)	2.541(3)
Nd(1)-O(7)#1	2.507(3)	Nd(2)-O(12)	2.385(4)
Nd(1)-O(8)	2.648(3)		

Symmetry Transformations used to generate equivalent atoms : for **II:** #1: -x+1,-y,-z+1; #2: -x,-y,-z+1; #3: -x+1,-y-1,-z+1; for **IIa:** #1: -x+1,-y+1,-z+1, #2: -x,-y+1,-z+1, #3 -x+1,-y,-z+1; for **III:** #1: -x+1,-y+1,-z+1, #2: -x+2,-y+1,-z+1, #3: -x+1,-y+2,-z+1.

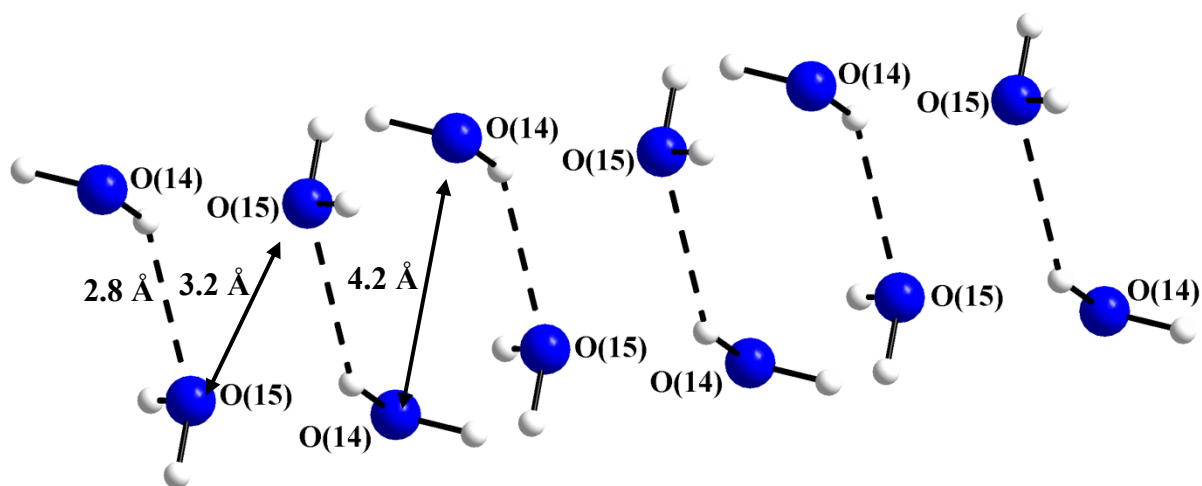**Table 3**: Important H-bonding interactions observed in the Pr compound

D – H . . . A	D – H, (Å)	H . . . A, (Å)	D – A, (Å)	D – H . . . A, (°)	Symmetry
O(1) – H(1A) . . . O(13)	0.97	1.63	2.5864	169	1-x,-y,1-z
O(11) – H(11A) . . . O(14)	0.99	1.72	2.6667	158	1-x,1-y,1-z
O(14) – H(14A) . . . O(13)	0.85	1.93	2.7707	172	x, y, 1+z
O(14) – H(14B) . . . O(15)	0.85	2.12	2.8466	143	2-x,1-y,-z
O(15) – H(15A) . . . O(4)	0.85	2.18	2.9794	156	1+x,y,z
O(15) – H(15B) . . . O(12)	0.85	2.40	3.2064	158	1-x,-y,1-z

(a)

(b)

(c)
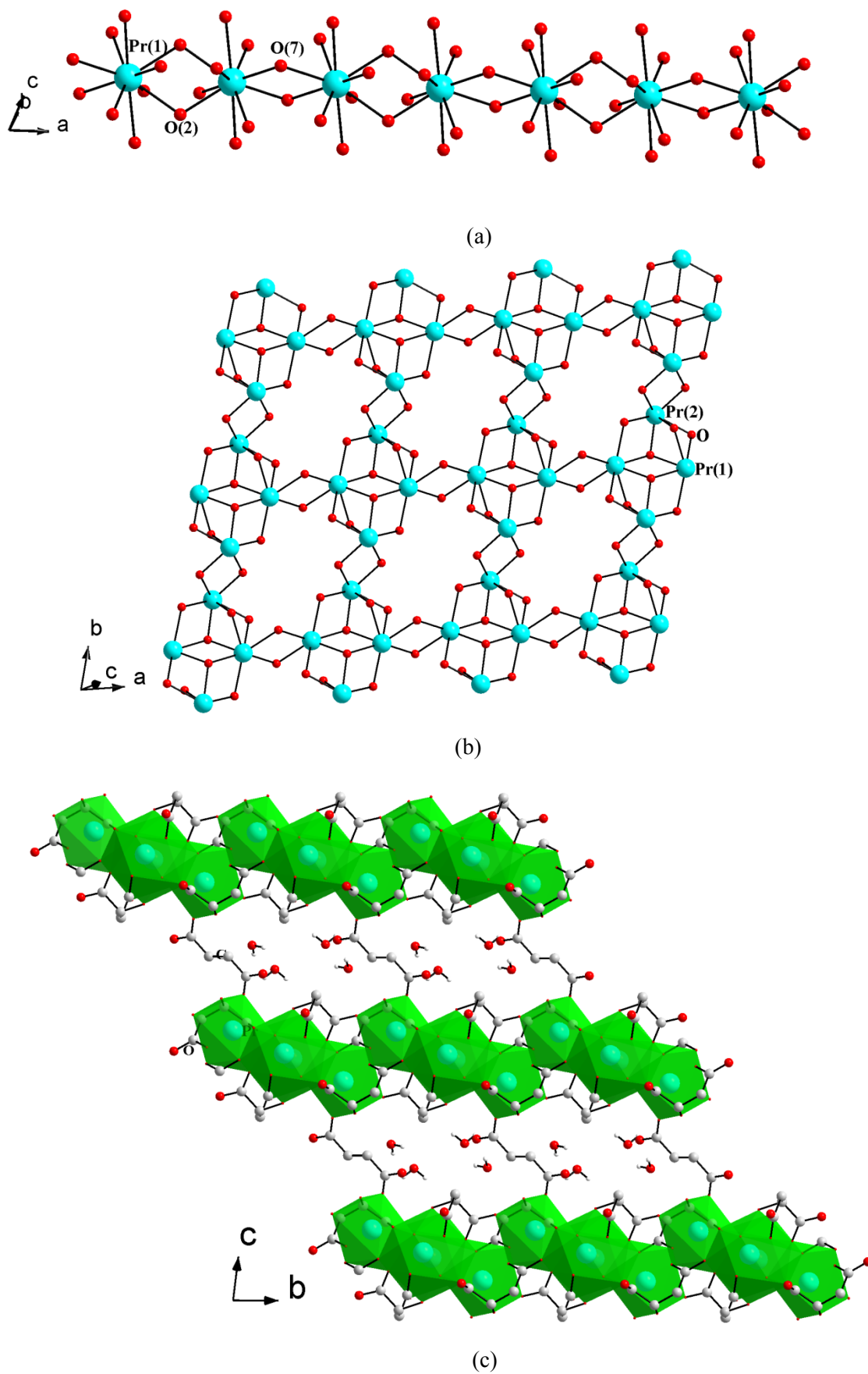
Sushrutha and Natarajan **Fig. 1**

(a)

(b)
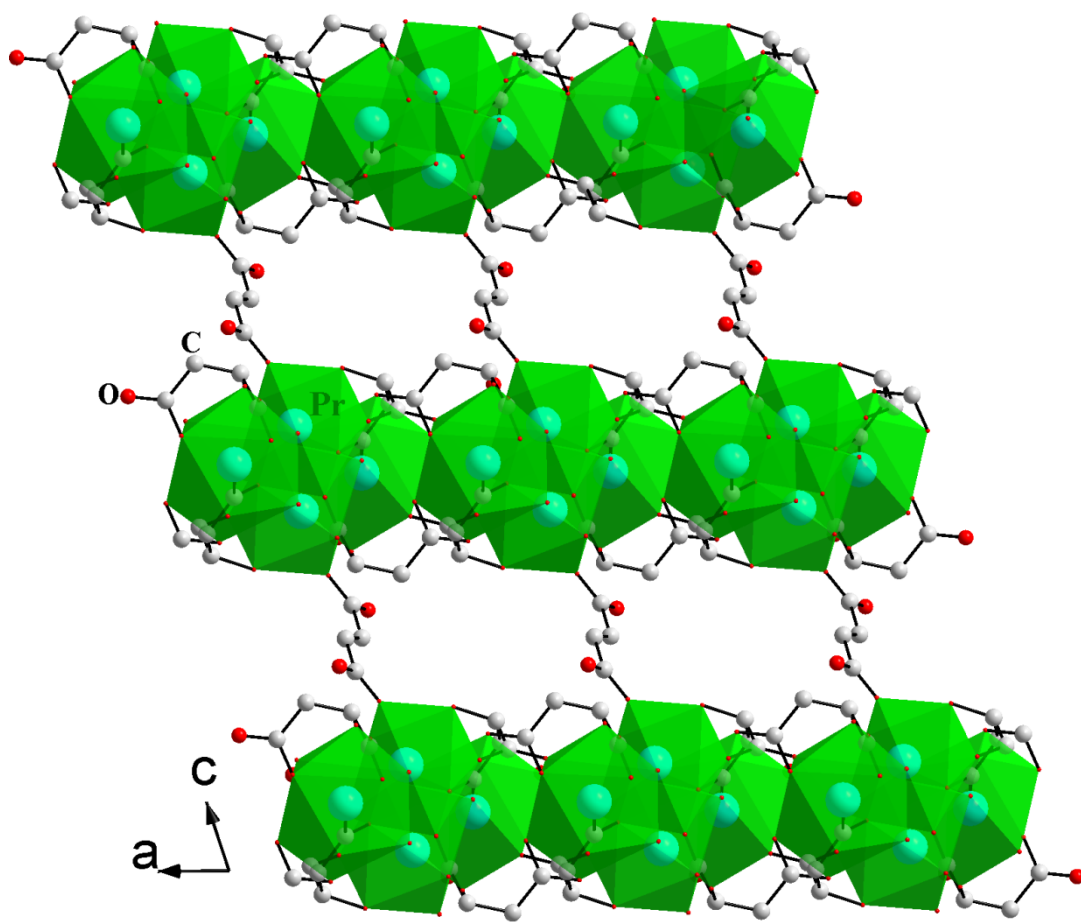
Sushrutha and Natarajan **Fig. 2**
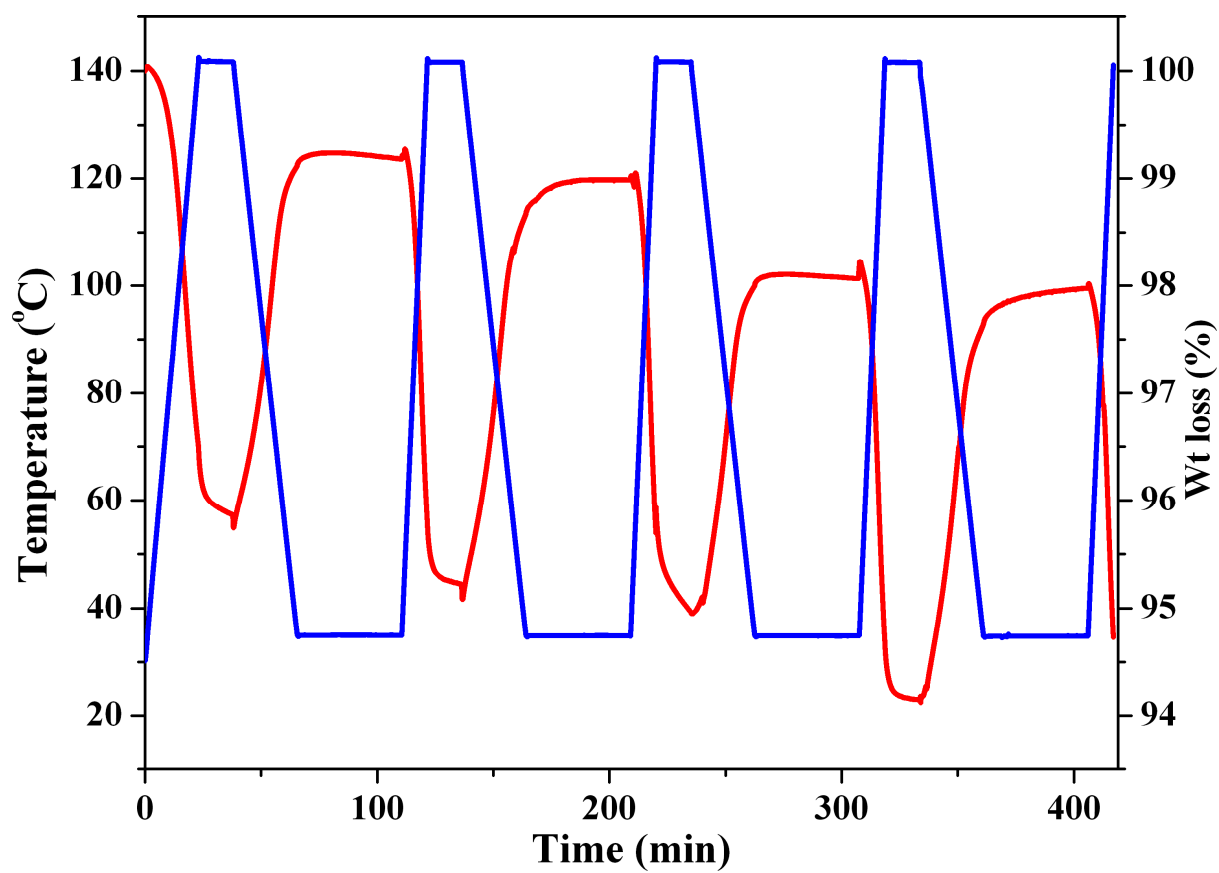
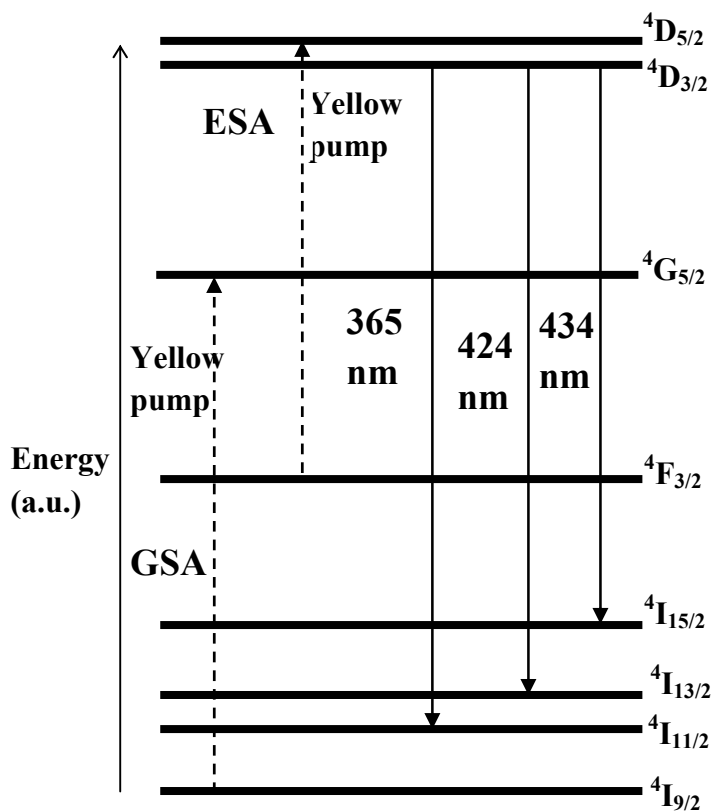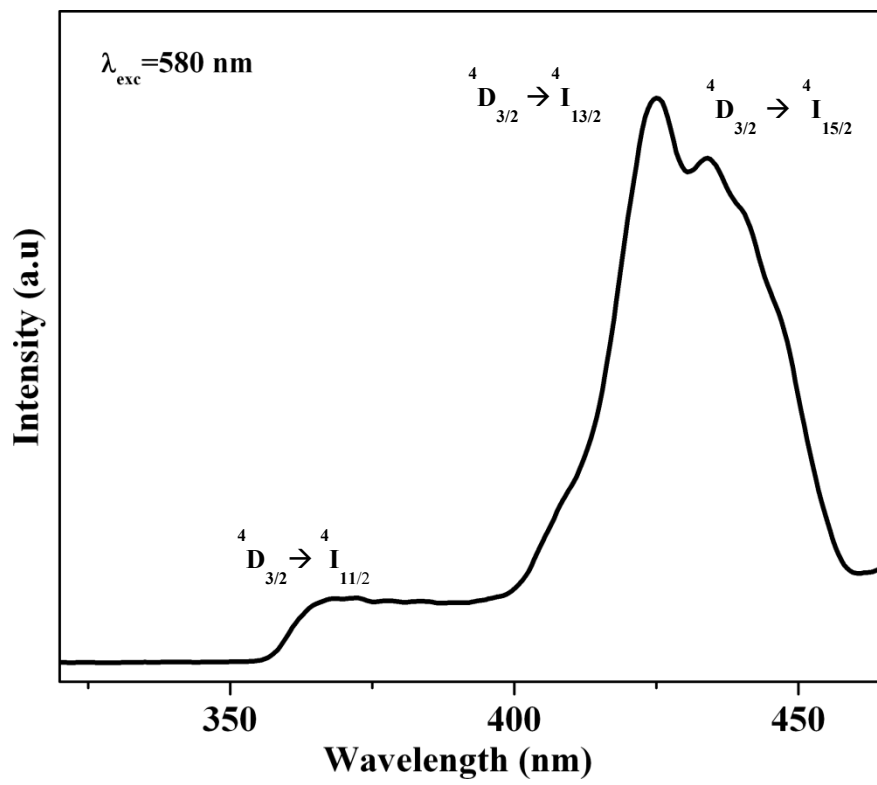Sushrutha and Natarajan **Fig. 3**
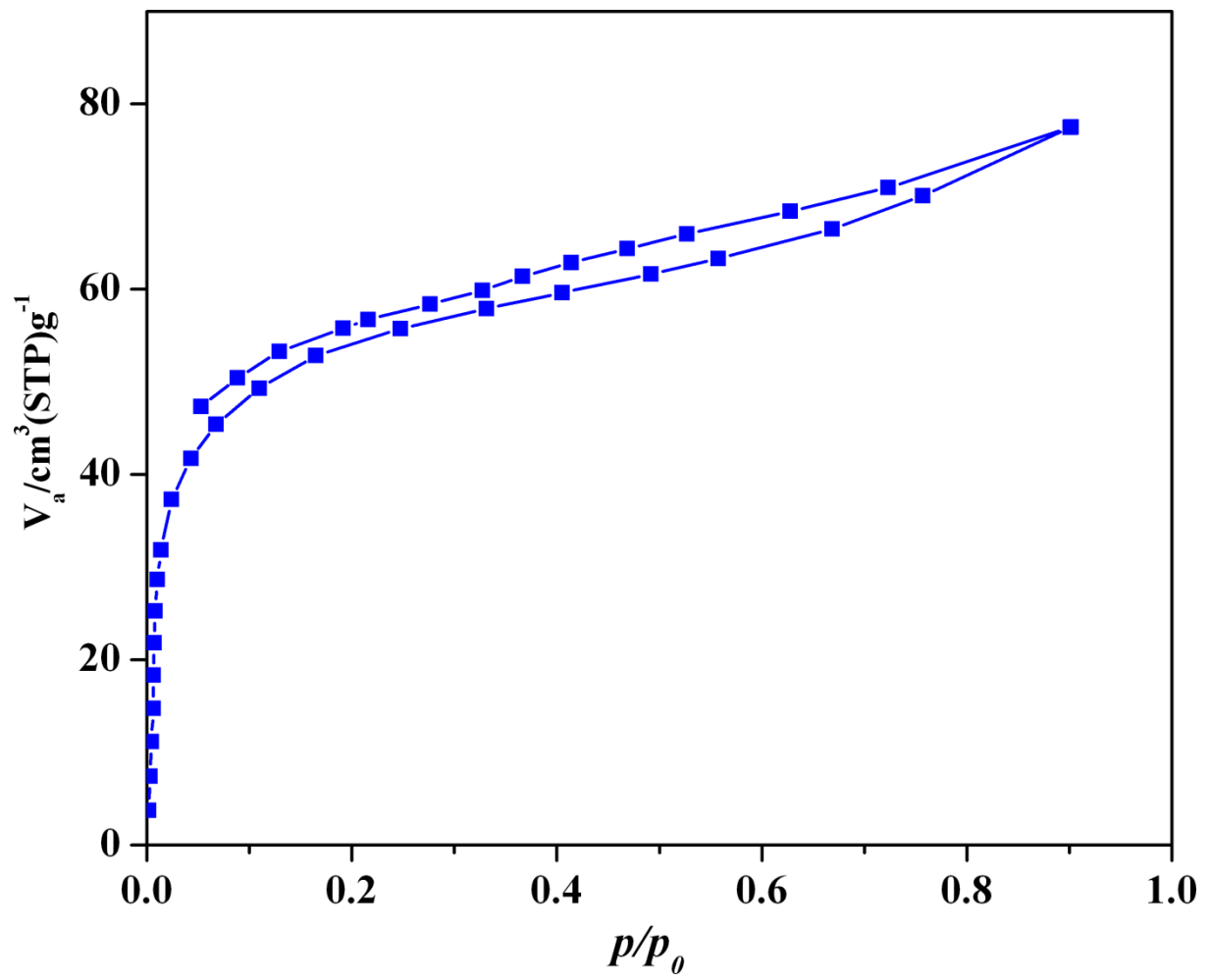
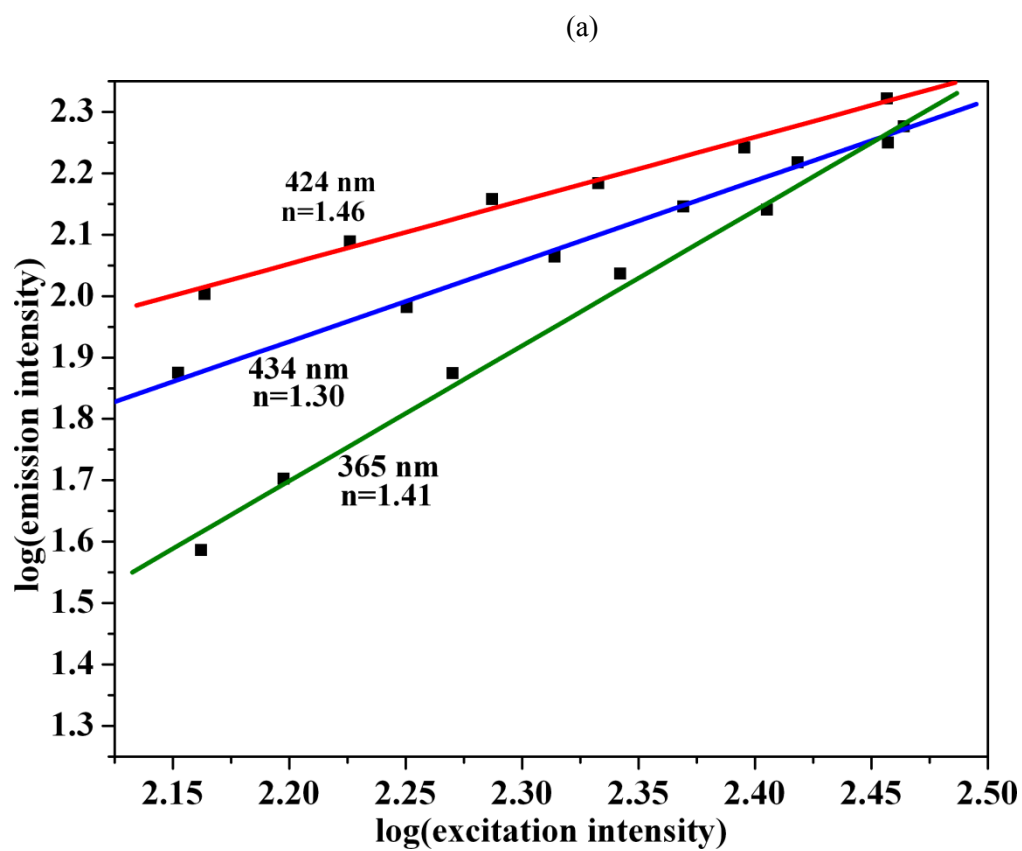Sushrutha and Natarajan **Fig. 4**

(a)

(b)
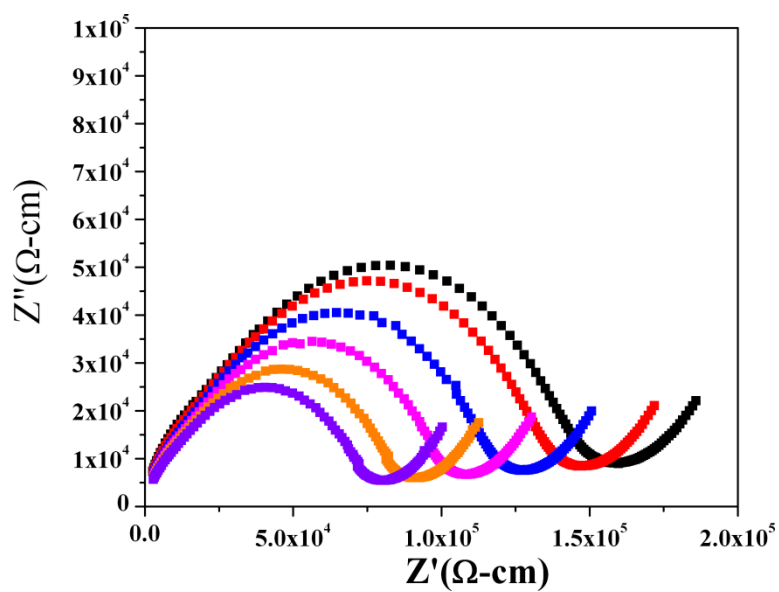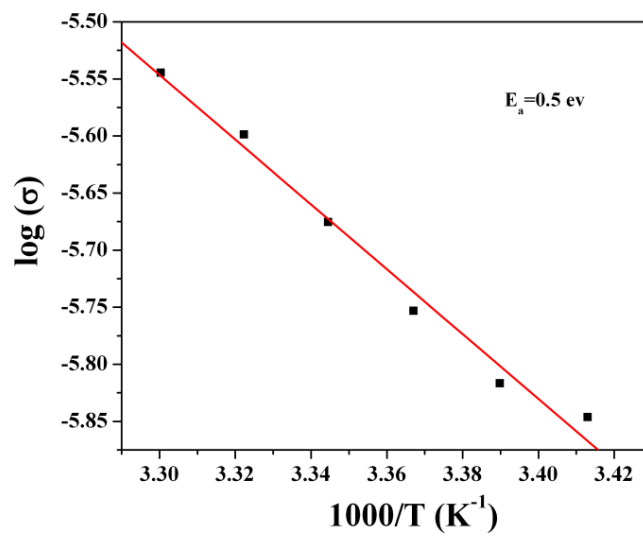
Sushrutha and Natarajan **Fig. 5**

(a)

(b)
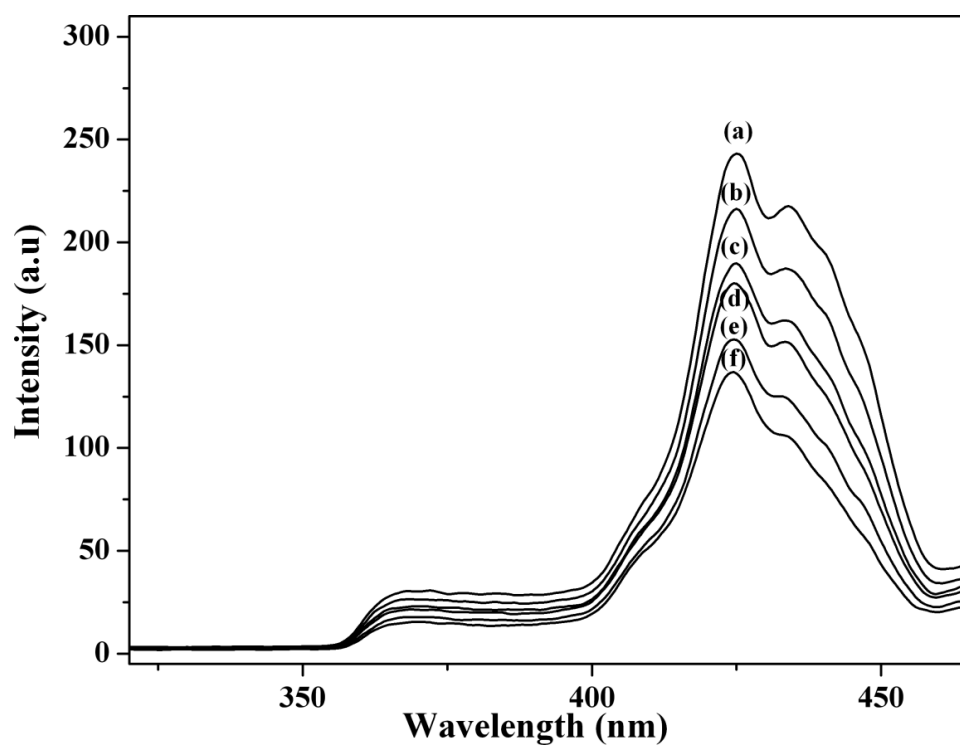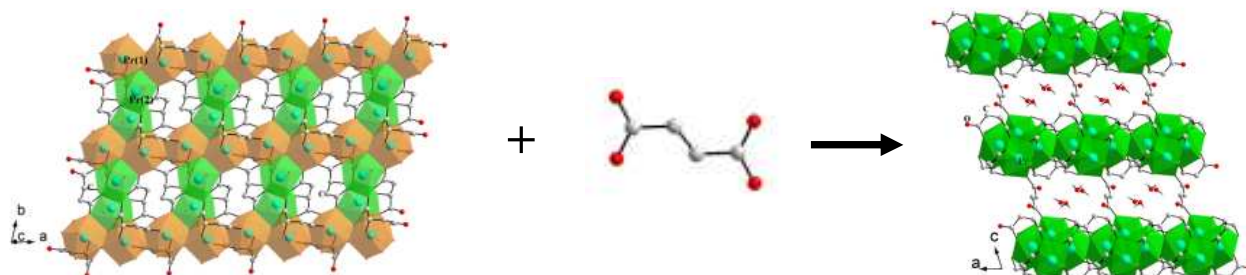
Sushrutha and Natarajan **Fig. 6**

23

Sushrutha and Natarajan **Fig. 7**

24

(a)

(b)
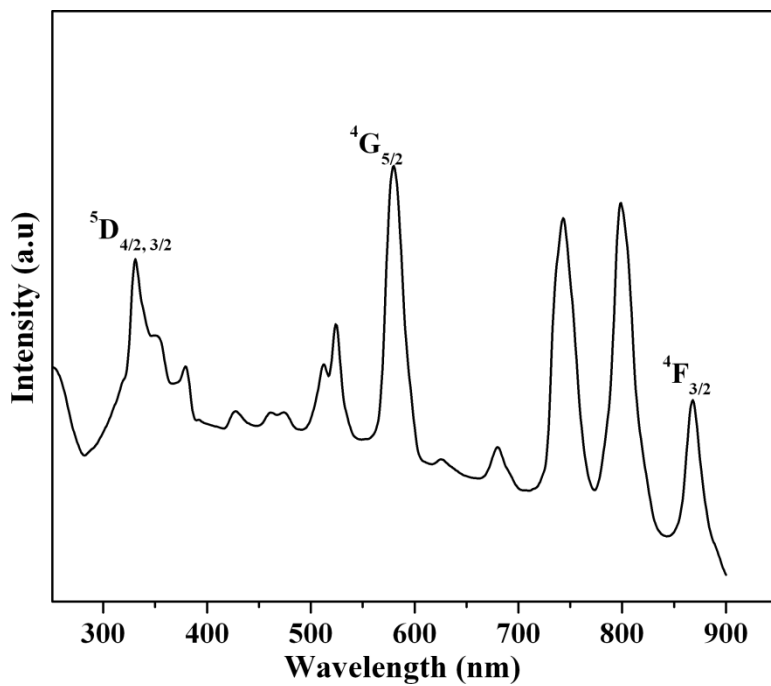
Sushrutha and Natarajan **Fig. 8**

Table of Contents

Three new three-dimensional hybrid compounds, $Ln_2(\mu_3\text{-OH})(C_4H_4O_5)_2(C_4H_2O_4)]. 2H_2O$, (Ln = Ce, Pr and Nd) ($I^2O^1$-type) exhibiting proton conductivity, multi-photon up-conversion behaviour has been described.